Hydrol. Earth Syst. Sci., 19, 1–13, 2015
www.hydrol-earth-syst-sci.net/19/1/2015/
doi:10.5194/hess-19-1-2015

Hydrology and Earth System Sciences
Open Access

Testing gridded land precipitation data and precipitation and runoff reanalyses (1982–2010) between 45° S and 45° N with normalised difference vegetation index data

S. O. Los

Department of Geography, Swansea University, Swansea SA2 8PP, UK

Correspondence to: S. O. Los (s.o.los@swansea.ac.uk)

Received: 2 September 2014 – Published in Hydrol. Earth Syst. Sci. Discuss.: 2 December 2014
Revised: 5 March 2015 – Accepted: 23 March 2015 – Published:

Abstract. The realistic simulation of key components of the land-surface hydrological cycle – precipitation, runoff, evaporation and transpiration, in general circulation models of the atmosphere – is crucial to assess adverse weather impacts on environment and society. Here, gridded precipitation data from observations and precipitation and runoff fields from reanalyses were tested with satellite derived global vegetation index data for 1982–2010 and latitudes between 45° S and 45° N. Data were obtained from the Climate Research Unit (CRU), the Global Precipitation Climatology Project (GPCP) and Tropical Rainfall Monitoring Mission (TRMM; analysed for 1998–2010 only) and precipitation and runoff reanalyses were obtained from the National Centers for Environmental Prediction/National Center for Atmospheric Research (NCEP/NCAR), the European Centre for Medium-Range Weather Forecasts (ECMWF) and the NASA Global Modelling and Assimilation Office (GMAO). Annual land-surface precipitation was converted to annual potential vegetation net primary productivity (NPP) and was compared to mean annual normalised difference vegetation index (NDVI) data measured by the Advanced Very High Resolution Radiometer (AVHRR; 1982–1999) and Moderate Resolution Imaging Spectroradiometer (MODIS; 2001–2010). The effect of spatial resolution on the agreement between NPP and NDVI was investigated as well. The CRU and TRMM derived NPP agreed most closely with the NDVI data. The GPCP data showed weaker spatial agreement, largely because of their lower spatial resolution, but similar temporal agreement. MERRA Land and ERA Interim precipitation reanalyses showed similar spatial agreement to the GPCP data and good temporal agreement in semi-arid regions of the Americas, Asia, Australia and southern Africa. The NCEP/NCAR reanalysis showed the lowest spatial agreement, which could only in part be explained by its lower spatial resolution. No reanalysis showed realistic inter-annual precipitation variations for northern tropical Africa. Inclusion of runoff in the NPP prediction resulted only in marginally better agreement for the MERRA Land reanalysis and slightly worse agreement for the NCEP/NCAR and ERA Interim reanalyses.

1 Introduction

Modelling the hydrological cycle in general circulation models (GCMs) of the atmosphere and numerical weather forecasting models is wrought with uncertainties. There is uncertainty in the estimation of precipitation rates associated with the representation of physical processes leading to droplet formation in clouds (Jonas, 1996; Randall, 2013) as well as in other components of the water balance – evaporation, transpiration and runoff. As a result water fluxes vary in magnitude among models (Jasechko et al., 2013, 2014; Coenders-Gerrits et al., 2014; Schlesinger and Jasechko, 2014). Yet, because of the crucial importance of water for society and the environment, it is important that the hydrological cycle is correctly represented.

In the present study three gridded precipitation data sets and three reanalysis precipitation and runoff products are tested. The precipitation data are the Climate Research Unit (CRU) time series (TS) version 3.21 data derived from gauge observations (Harris et al., 2014), the Global Precipitation Climatology Project (GPCP) version 2.2 data de-

rived from a joint analysis of satellite data and gauge data (Huffman et al., 2009) and the Tropical Rainfall Monitoring Mission (TRMM) 3B43 and 3A12 monthly data. Full years of TRMM data were only available from 1998 onward. The three precipitation and runoff products tested are from the National Centers for Environmental Prediction/National Center for Atmospheric Research (NCEP/NCAR) reanalysis (Kalnay et al., 1996), the European Centre for Medium-Range Weather Forecasts Interim Reanalysis (ERA Interim) (Berrisford et al., 2011) and the NASA Global Modeling and Assimilation Office (GMAO) Modern Era Retrospective-analysis for Research and Applications (MERRA) Land reanalysis (Reichle et al., 2011).

The precipitation and precipitation minus runoff fields are evaluated by first calculating annual potential water limited net primary productivity (NPP). NPP, the net amount of carbon absorbed by vegetation from the atmosphere through photosynthesis, is compared with satellite observed normalised difference vegetation index (NDVI) data to which it is closely linked (Tucker and Sellers, 1986; Potter et al., 1993). This approach has the advantage that precipitation fields are tested on independent data over large areas where precipitation data are sparse. Testing reanalyses on precipitation data may not be an independent test since precipitation data are frequently assimilated in reanalyses.

In the present study NPP, derived from both precipitation and precipitation minus runoff, is compared with NDVI for the period of 1982–2010. The comparisons are limited to the land surface between 45° S and 45° N, where correlations between precipitation and vegetation net primary productivity or vegetation index are high. Both spatial and temporal comparisons are made between water (precipitation or precipitation minus runoff) limited NPP and NDVI. Since precipitation fields have different spatial resolutions, comparisons are made for the spatial resolution at which the data are distributed as well as for the spatial resolution of the NCEP/NCAR reanalysis (1.875° × 1.875°).

The paper is organised as follows: in Sect. 2 the vegetation index data, precipitation data and precipitation and runoff reanalyses are briefly discussed. In Sect. 3 the estimation of NPP from annual precipitation and annual precipitation minus runoff is described. The effects of errors in NPP of relevance for the present analysis are discussed. Section 4 provides the results of the spatial and temporal comparisons of NPP with NDVI and highlights examples where large deviations exist. The effect of scale on agreement between NDVI and NPP is investigated as well. Section 5 provides a discussion of the results.

2 Data

2.1 Normalised difference vegetation index data

2.1.1 FASIR NDVI

The Fourier adjusted, solar and sensor zenith angle corrected, interpolated and reconstructed (FASIR) normalised difference vegetation index (NDVI) data were derived from Advanced Very High Resolution Radiometer (AVHRR) data for 1982–1999 and from MODIS data for 2000–2010 (Los, 2013). The AVHRR data were corrected for sensor degradation (Los, 1993, 1998), atmospheric ozone absorption and molecular scattering (James and Kalluri, 1994), scattering and absorption by stratospheric aerosols (Los et al., 2000), bidirectional reflectance distribution function (BRDF) effects which vary with sensor viewing zenith angle and solar zenith angle (Los et al., 2005), and missing data and erroneous data caused by cloud contamination and short-term atmospheric effects (Los et al., 2000; Sellers et al., 1996). The Moderate Resolution Imaging Spectroradiometer (MODIS) data were calibrated to a common standard, corrected for atmospheric aerosols, water vapour, scattering and view zenith angle effects (Vermote et al., 2001; Huete et al., 2002). A Fourier adjustment was applied to the MODIS data, similar to the one applied to the AVHRR data (Sellers et al., 1996; Los, 2013). MODIS monthly means and variances were adjusted to be similar to the AVHRR data (Los, 2013). The MODIS data were not corrected for solar zenith angle effects, which introduces a small, consistent seasonal error in the data that is partly accounted for by the normalisation of the MODIS data to the AVHRR data. Variations between years should not be affected since the time of overpass of MODIS, and therefore the solar zenith angles at the time of observation are the same from year to year. FASIR NDVI data were interpolated to the respective spatial resolutions of the precipitation data and precipitation reanalyses.

2.2 Precipitation data

2.2.1 Climate Research Unit (CRU) TS 3.21 precipitation

CRU time series (TS) 3.21 precipitation data at 0.5° × 0.5° spatial resolution were used (Harris et al., 2014). Spatial interpolation of station data to obtain gridded data for the entire land surface is based on interpolation of monthly anomalies from the 1961–1990 climatology (Harris et al., 2014). Monthly CRU data were summed to obtain annual precipitation for 1982–2010.

2.2.2 Global precipitation climatology project (GPCP) precipitation

Monthly GPCP data version 2.2 is a merged analysis of satellite data and rain gauge data (Huffman et al., 2001, 2009,

2011). The GPCP data were interpolated to $0.5° \times 0.5°$ and summed to obtain annual rainfall values for 1982–2010.

2.2.3 Tropical Rainfall Monitoring Mission (TRMM) precipitation

The aim of TRMM is to measure rainfall between latitudes of 40° S and 40° N and thereby fill important gaps in the (land and ocean) surface precipitation gauge record. The 3B43 data have $0.25° \times 0.25°$ spatial resolution, a monthly time step and cover latitudes between 50° S and 50° N. The data combine the TRMM satellite data with data from the GPCP ground station network and with data from sensors aboard the Aqua, Terra, Defence Meteorological Satellite Program and NOAA satellites (Huffman et al., 2007, 2010). The 3B43 data were averaged to the $0.5° \times 0.5°$ resolution of the FASIR NDVI data. TRMM 3A12 data, a monthly $0.5° \times 0.5°$ data set between 40° S and 40° N based on TRMM data only, were analysed as well. The 3A12 data analysis is limited since these showed a poor agreement with other data for the land surface (Sect. 4.1).

2.3 Precipitation reanalyses

2.3.1 National Centers for Environmental Prediction/National Center for Atmospheric Research (NCEP/NCAR)

The NCEP/NCAR reanalysis is one of the oldest reanalysis products available. The record goes back until 1948 and is updated in near real time (Kalnay et al., 1996). Daily surface Gaussian precipitation rates and runoff ($\mathrm{kg\,m^{-2}}$) at $1.875° \times 1.875°$ resolution were converted to total annual totals ($\mathrm{mm\,yr^{-1}}$).

2.3.2 European Centre for Medium-Range Weather Forecasting (ECMWF) Interim reanalysis (ERA Interim)

ERA Interim reanalysis is available from 1979 until the near present at a spatial resolution of $0.75° \times 0.75°$. Synoptic monthly means of total precipitation were obtained and were converted to total annual precipitation ($\mathrm{mm\,yr^{-1}}$). Data were analysed at $0.75° \times 0.75°$ and $1.875° \times 1.875°$ resolutions.

2.3.3 Modern-era retrospective analysis for research and applications reanalysis

The MERRA reanalysis and MERRA Land reanalysis were produced by the Global Modelling and Analysis Office (GMAO) at NASA/Goddard Space Flight Center. The MERRA reanalysis and MERRA Land reanalysis differ; the latter assimilates the GPCP precipitation data and uses an improved hydrological model (Reichle et al., 2011). Both the MERRA reanalysis and MERRA Land reanalysis have a spatial resolution of $0.67° \times 0.5°$ (longitude $\times$ latitude). Precipitation and runoff were summed to annual values ($\mathrm{mm\,yr^{-1}}$). Only the MERRA Land reanalysis was used in the present study. Data were analysed at $0.67° \times 0.5°$ and $1.875° \times 1.875°$ resolutions.

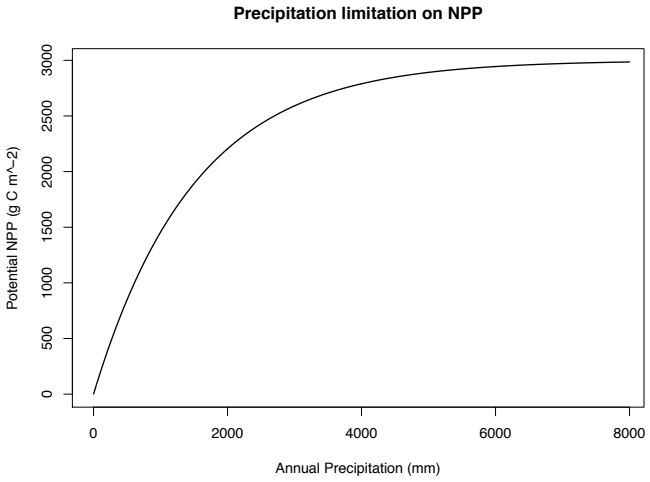

Figure 1. Lieth's net primary production (NPP) model describing potential NPP ($\mathrm{g\,C\,m^{-2}\,yr^{-1}}$) as a function of annual precipitation. This model, as used in the present study, ignores other environmental limitations caused by, e.g., temperatures, soil properties, and solar radiation.

3 Analysis

Annual gridded precipitation data and annual precipitation reanalysis products (all six in $\mathrm{mm\,y^{-1}}$) are converted to annual potential net primary productivity (NPP in $\mathrm{g\,C\,m^{-2}\,yr^{-1}}$), i.e. the net amount of carbon absorbed by land-surface vegetation from the atmosphere over a year limited by water availability only. Annual precipitation limited NPP is calculated using Lieth's model (Esser et al., 1994):

$$\mathrm{NPP_P} = 3000\{1 - \exp(-0.000664\,P)\} \quad (1)$$

with

$\mathrm{NPP_P}$ = annual precipitation limited NPP

P = annual precipitation ($\mathrm{mm\,yr^{-1}}$).

In a statistical sense Lieth's model can be seen as a data transformation where NPP increases linearly with precipitation at low values; at higher values the increase in NPP with precipitation becomes smaller until it reaches an upper limit near $5000\,\mathrm{mm\,yr^{-1}}$ (Fig. 1). The spatial distributions of annual precipitation limited potential NPP for the six precipitation products analysed are shown in Fig. 2.

NPP is near-linearly linked to mean annual NDVI as follows (Kumar and Monteith, 1982; Potter et al., 1993):

$$\mathrm{NPP} = \epsilon\, f_{\mathrm{APAR}} \times \mathrm{PAR} \quad (2)$$

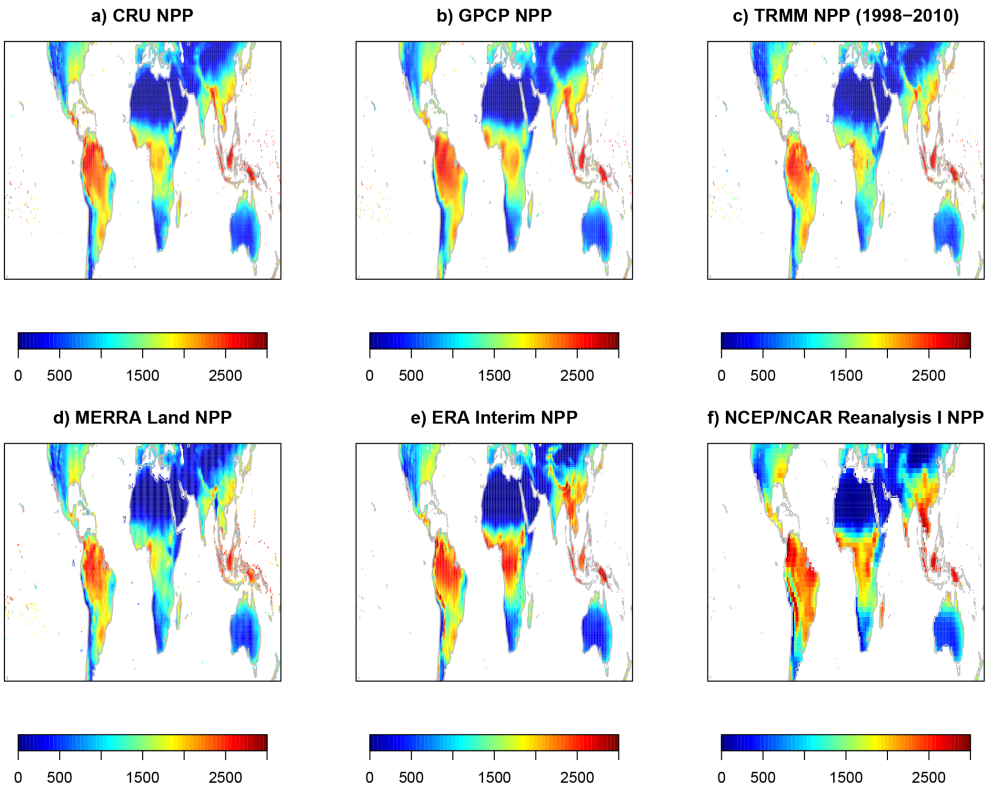

Figure 2. Spatial distribution of mean potential rainfall limited NPP fields derived from Lieth's model (Fig. 1). **(a)** Mean annual precipitation limited NPP for 1982–2010 from CRU data. **(b)** NPP for GPCP data, **(c)** NPP for TRMM 3B43 data, average calculated over 1998–2010, **(d)** NPP for MERRA Land reanalysis, **(e)** NPP for ERA Interim reanalysis and **(f)** NPP for NCEP/NCAR Reanalysis I.

with

ϵ = environment-dependent efficiency factor

PAR = photosynthetically active radiation

f_{APAR} = fraction of PAR absorbed by green parts of vegetation.

Since the f_{APAR} is near-linearly related to NDVI (Tucker and Sellers, 1986), a near linear relationship is expected between NPP and NDVI (Potter et al., 1993; Malmström et al., 1997).

The error in NPP (Eq. 1) can be expressed as a sum of component errors:

$$\eta = \left(\eta_{\mathrm{P}}^2 + \eta_{\mathrm{E}}^2 + \eta_Q^2 + \eta_{\mathrm{G}}^2 + \eta_{\mathrm{T}}^2 + \eta_{\mathrm{I}}^2 + \eta_{\Delta \mathrm{S}} + \ldots\right)^{0.5}, \qquad (3)$$

where η is the total error in NPP which consists of errors in the gridded precipitation data or reanalysis products (η_{P}). The investigation of the error η_{P} is the objective of the present study. Other error terms are related to ignoring components of the water budget in Eq. (1). These are evaporation from soils and intercepted rainfall (η_E), runoff (η_{Q}), and infiltration to ground water (η_{G}). These components of the water budget are effectively "lost" to vegetation; i.e. these components are not taken up by plants and are transpired into the atmosphere. Errors associated with other factors not incorporated in Eq. (1) are limitations posed on vegetation by temperature (η_{T}), solar radiation η_{I} and changes in soil and groundwater storage $\eta_{\Delta S}$. The list of errors in Eq. (3) is not exhaustive and other errors (...), such as caused by ignoring differences in water use between C3 and C4 species, may affect the analysis. Under the assumption that errors are additive (Eq. 3), a smaller error in η_{P} will lead to a smaller error in η since other errors are the same. Thus the key assumption here is that lower errors in η_{P} will lead to lower errors in NPP and improved statistics such as higher correlations between NDVI and NPP and a smaller root mean square error (E_{RMS} s).

The analysis is limited to the land surface between 45° S and 45° N. At these latitudes water is limiting vegetation growth and the association among precipitation, NPP and NDVI is therefore high. As a result, the precipitation error term in Eq. (3), η_{P}, is large compared to the other error terms. Exceptions are high-altitude areas where temperature is likely limiting plant growth, or areas where increased cloudiness and increased precipitation are linked with decreased solar radiation. In these areas lower or even negative correlations between precipitation and vegetation greenness may be expected.

Equation (3) shows that incorporation of more components in Eq. (1), e.g. components of the water budget, should

reduce, or at least not increase, the overall error in η. This provides a way to evaluate other components of the water budget such as runoff (Sect. 4.2). If simulations of runoff are realistic, the NPP fields calculated from annual precipitation minus runoff ought to be closer to the observed NDVI values than the NPP fields calculated from annual precipitation. The evaluation of precipitation minus runoff is necessarily limited to the reanalyses since the CRU, TRMM and GPCP data do not contain runoff estimates. NPP from precipitation minus runoff is calculated using a modified form of Eq. (1).

$$\mathrm{NPP_{P-Q}} = 3000 \times \left\{1 - \exp\left[\frac{-0.000664 \times (P-q)}{f}\right]\right\} \quad (4)$$

with

$f = \widetilde{P-q}/\widetilde{P}$

$\widetilde{P-q} =$ median $P-q$ for 1982–2010 and 45° S–45° N

$\widetilde{P} =$ median P for 1982–2010 and 45° S–45° N.

The value for f varies between reanalysis products; $f_{\mathrm{MERRA}} = 0.95$, $f_{\mathrm{ERA}} = 0.89$ and $f_{\mathrm{NCEP}} = 0.894$. A value of $f = 0.892$ is used, which is in the middle of the two closest median f values. Results for MERRA NPP calculations did not change when a value of $f = 0.95$ was used.

3.1 Spatial and temporal correlation analysis

The precipitation limited NPP fields are compared spatially and temporally with NDVI. For the spatial comparison, correlations are calculated between NPP and NDVI spatial fields of the same year, resulting in time series with one correlation coefficient for each year. For the temporal comparison correlations are calculated between NPP and NDVI time series, resulting in a spatial distribution of correlation coefficients with one correlation coefficient for each cell.

4 Results

The results are presented in two subsections. In Sect. 4.1 the analysis of precipitation data and reanalyses is presented. This includes the analysis of spatial correlations through time, the exploration of residual errors (biases and root mean square errors) and the analysis of gridded correlations between NPP and NDVI time series. Examples are highlighted of problems revealed by the spatial and temporal correlation analysis. In Sect. 4.2 the precipitation minus runoff reanalyses are analysed.

4.1 Testing gridded precipitation fields

4.1.1 Spatial comparison of precipitation derived NPP with NDVI

The spatial correlations between annual NDVI and precipitation limited annual NPP from CRU and GPCP data, and

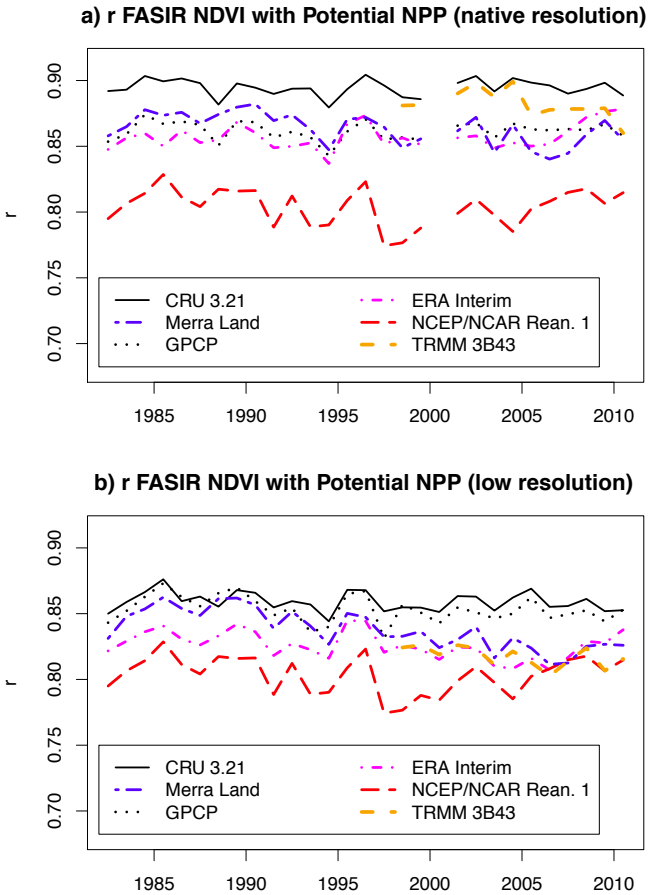

Figure 3. Spatial correlation for 1982–2010 between mean annual FASIR NDVI and potential annual NPP for six precipitation products. Correlations are calculated for the entire land surface between 45° S and 45° N and indicate spatial agreement between rainfall patterns and the vegetation index. Highest correlations are found for CRU NPP, lowest for MERRA (not MERRA Land) NPP ($0.611 < r < 0.681$; not shown). **(a)** Correlations at native resolution of precipitation data. **(b)** Correlations with data scaled to NCEP/NCAR resolution (1.875° × 1.875°).

MERRA Land, NCEP/NCAR and ERA Interim reanalyses are shown in Fig. 3a. Spatial correlations are the highest for the CRU data ($r \approx 0.89$) and TRMM data ($r \approx 0.88$), and the lowest for the NCEP/NCAR reanalysis ($r \approx 0.8$). Spatial correlations for the GPCP data and ERA Interim and MERRA Land reanalyses are clustered in a group with intermediate correlations ($r \approx 0.87$). Year-to-year variations in spatial correlations are the highest for the NCEP/NCAR reanalysis and are lower for the other data. The correlations for the MERRA (not MERRA Land) precipitation product are not shown, but were the lowest; the range for 1982–1999 was $0.611 < r < 0.681$.

The spatial correlations for the NPP fields at 1.875° × 1.875° resolution show the same order as the analysis on native-resolution NPP fields, but are lower if the resolution

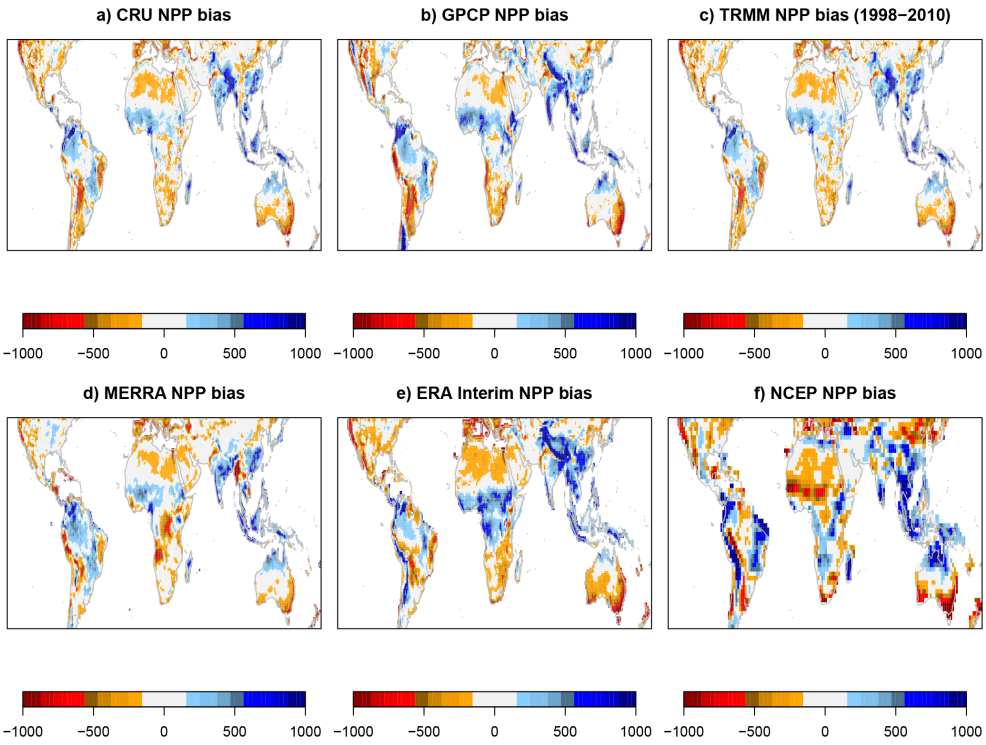

Figure 4. Mean deviation (bias) from the model $\mathrm{NPP}_P - (\beta_1 \mathrm{NDVI})$ for the years 1982–1999 and 2001–2010. **(a)** CRU data, **(b)** GPCP data, **(c)** TRMM data (1998–2010 only), **(d)** MERRA Land reanalysis, **(e)** ERA Interim reanalysis and **(f)** NCEP/NCAR reanalysis. The ERA Interim shows a large positive bias for tropical regions in Africa compared to the CRU and GPCP, but patterns for other continents are similar. The NCEP/NCAR reanalysis shows a consistently larger bias than the CRU and GPCP data for most vegetated areas.

decreases (Fig. 3a and b). For the lower resolution, CRU derived NPP has similar spatial correlations as GPCP NPP and TRMM NPP; the lower correlations of the GPCP data can therefore largely be attributed to their lower spatial resolution. The spatial correlation of the low-resolution MERRA, TRMM and ERA Interim NPP appears to decrease from the late 1990s; this is not shown to the same extent in the high-resolution correlations.

The spatial distribution of residuals from a simple regression model was explored, the regression model explaining all land-surface NPP values between 45° S and 45° N for 1982–2010 as a function of NDVI. The equation is given by

$$\mathrm{NPP} = \beta_1 V \tag{5}$$

with

$V = \mathrm{NDVI}$

$\beta_1 =$ the slope.

The regression model was applied to data for the AVHRR and MODIS periods combined (1982–1999 and 2001–2010), leaving out 2000. Figure 4 shows the mean deviations from the regression model. The smallest mean deviations are found in the CRU, GPCP and TRMM (1998, 1999 and 2001–2010) NPP fields. These deviations are in part caused by errors in precipitation data and factors ignored in the NPP model and provide a baseline against which other deviations are compared. Slightly higher deviations than for the CRU, TRMM and GPCP data are found in the MERRA NPP fields, in particular in the Amazon and in African tropical regions. The highest deviations are found in the ERA Interim (Africa, Asia) and NCEP/NCAR (throughout low latitudes) NPP fields. Notice that the NCEP/NCAR and ERA Interim NPP have mean deviations of opposite sign in the regions south of the Sahara. Figure 5 shows the spatial distribution of the root mean square error (E_{RMS}); the distribution of the E_{RMS} values largely agrees with the distribution of the mean deviations from the regression model, indicating that the E_{RMS} is explained by large structural location-dependent deviations.

4.1.2 Temporal comparison of precipitation derived NPP with NDVI

The spatial distributions of temporal correlations between NDVI and each of the five NPP products are shown in Fig. 6. Annual fields of NPP values between 45° S and 45° N were correlated with annual mean FASIR NDVI for 1982 until 1999 and 2001 until 2010. The year 2000 was left out of the evaluation because it was a transition year between the

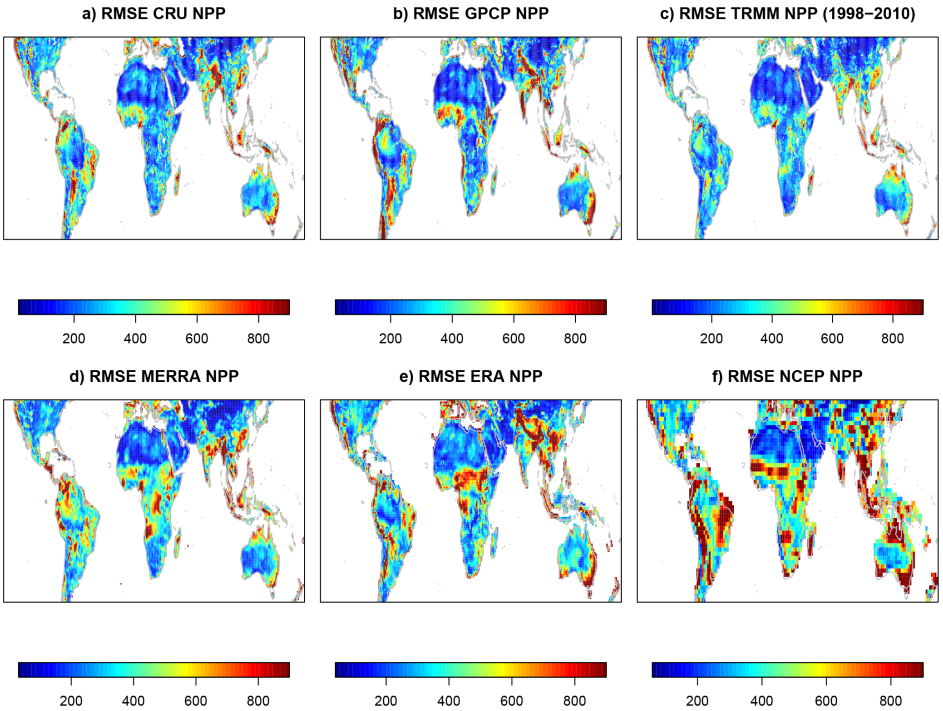

Figure 5. Root mean square error (E_{RMS}) from the model $\mathrm{NPP}_P - (\beta_1 \mathrm{NDVI})$ for the years 1982–1999 and 2000–2010. **(a)** CRU data, **(b)** GPCP data, **(c)** TRMM data, **(d)** MERRA Land reanalysis (showing larger E_{RMS} throughout), **(e)** ERA Interim reanalysis showing a large E_{RMS} south of the Sahara, and **(f)** NCEP/NCAR reanalysis.

AVHRR and MODIS data, and the MODIS record for this year is not complete.

The spatial coverage of positive correlations GPCP and CRU NPP fields are similar and are the highest of all NPP products. The GPCP NPP exhibits slightly higher correlations across northern Africa's semi-arid regions and slightly lower correlations for parts of the Amazon. The correlations for the NPP from precipitation reanalyses were similar to the correlations for the observations in the Americas, parts of Australia and southern Africa. Correlations for the northern tropical regions of Africa are poor for all reanalysis products and in some cases significant negative correlations were found between precipitation limited NPP and NDVI (Fig. 6c–e). Since the TRMM period covers only part of the record, the TRMM NPP correlations for 1998–2010 were compared with the CRU NPP correlations and were found to be slightly but significantly higher (Fig. 6f).

4.1.3 Temporal deviations in tropical northern Africa

Areas with negative temporal correlations between NPP and NDVI in the CRU and GPCP NPP were found in the eastern half of the Sahara north of the Sahel (centred at 17.75° N, 22.25° E; see Fig. 6a and b). Although of little consequence, it is interesting to explore this minor feature in more detail. This is done in Fig. 7 which shows two precipitation and two NDVI time series; one for the area in the Sahara where the positive correlation occurs (centred at 17.75° N, 22.25° E) and the other a couple of degrees further south of the Sahara (centred at 15.25° N, 22.25° E). Also shown in the figure (Fig. 7b) is the correlation of the southernmost precipitation time series with precipitation time series along a south–north transect. This correlation gradually decreases to zero over a distance of about 10° latitude. By contrast, the same correlation for the NDVI time series (Fig. 7c decreases much faster to zero, over 2.5° latitude (Fig. 7d)). This indicates that the interpolation of precipitation data for the Sahel should use a much shorter north–south correlation distance.

Of greater consequence than the previous issue is the lack of significant positive correlations in northern parts of tropical Africa for all reanalyses. Averaged precipitation time series for two areas directly south of the Sahara highlight several problems (Fig. 8). The most important one is that the drought of the century in 1984 and the subsequent recovery of rainfall in the Sahel is not correctly represented in any of the precipitation reanalyses. By comparison, the CRU and GPCP precipitation data correctly show the 1984 drought and the subsequent recovery resulting in an overall upward trend for later years (Fig. 8a and b). The NCEP/NCAR reanalysis is overall too low both for the western and eastern parts south of the Sahara, but does show similar interannual variations for 1982–1997 and an overall positive trend. This positive trend appears too large for the last 5 years of the record. The MERRA Land precipitation does not show a trend and does

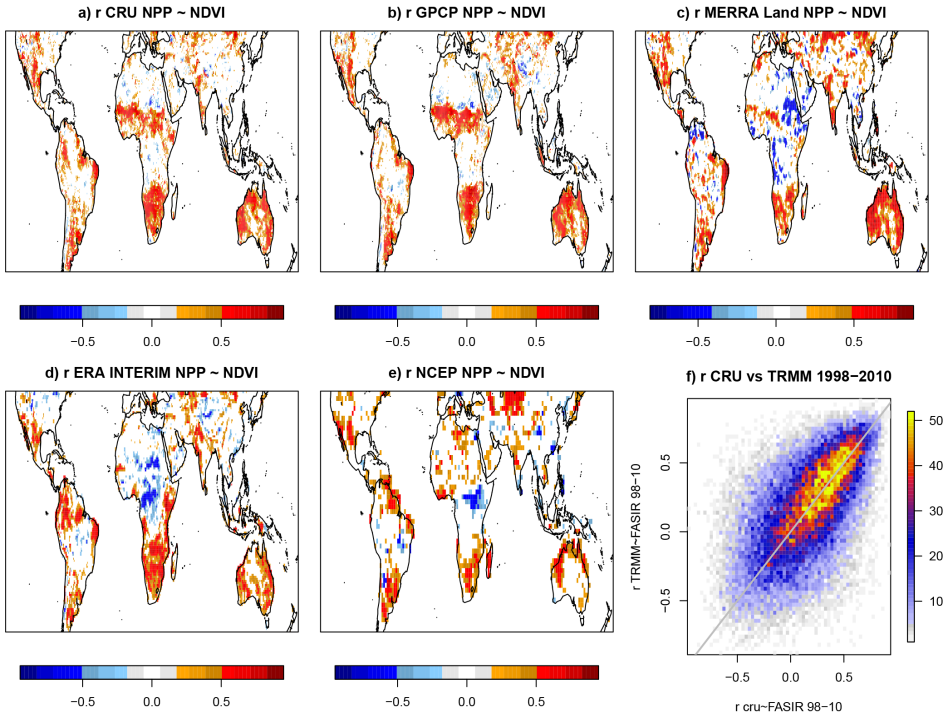

Figure 6. Spatial distributions of correlations (significant at $p < 0.1$) between NDVI time series and potential NPP time series calculated from annual precipitation amounts for 1982–2010 (2000 excluded). **(a)** Correlations for CRU data, **(b)** GPCP data, **(c)** MERRA Land reanalysis, **(d)** ERA Interim reanalysis and **(e)** NCEP/NCAR reanalysis. **(f)** Density scatter plot of correlations for the CRU and TRMM (version 3B43) data for the periods of 1998 and 2010 (all (significant and not significant) correlations included; grey line is the 1 : 1 line). The mean correlation for TRMM 3B43 data ($r = 0.188$) was significantly higher ($p = 0.0033$) than for CRU data ($r = 0.181$). The mean temporal correlation for TRMM 3A12 data ($r = 0.115$) between 40° S and 40° N was significantly lower (note: agreement between TRMM 3A12 and 3B43 was higher over oceans – not shown). All reanalysis products **(c–e)** show poor correlations for the Sahel and savanna regions south of the Sahara. Notice areas with negative correlations in the south-eastern parts of the Sahara in the CRU **(a)** and GPCP **(b)** data (see also Fig. 7).

not identify 1984 as the year with the largest drought, despite the assimilation of GPCP data in this product. The ERA Interim precipitation shows a negative trend from 1982 to 2010 for the western part. For the eastern area (Fig. 8b), the ERA interim precipitation shows huge deviations in precipitation that persist for multiple years (e.g. 1990 until 1998). Deviations in the ERA Interim precipitation, both positive and negative, are much larger than in the observations.

4.2 Testing precipitation minus runoff

The NCEP/NCAR, ERA Interim and MERRA Land reanalyses provide estimates of surface runoff. Runoff is effectively lost to vegetation, and therefore the difference between precipitation and runoff should be more closely linked to NPP than precipitation. NPP was calculated from precipitation minus runoff using Eq. (4). An analysis of spatial and temporal correlations is presented for NPP fields calculated from precipitation minus runoff, similar to those calculated from precipitation (Sect. 4.1).

Figure 9a shows the temporal variation in the spatial correlation between NDVI and NPP calculated from precipitation minus runoff for the three reanalyses. Compared to the analysis of NPP from precipitation, the average improvement in the correlation with NDVI for the MERRA land precipitation minus runoff NPP is 0.01 (Fig. 9b). The ERA Interim shows an overall decrease in spatial correlation (−0.024), but does show a dramatic improvement for the last couple of years; here the analysis shows a similar improvement in correlation to the MERRA Land NPP. The NCEP/NCAR precipitation minus runoff NPP shows a larger decrease in correlation (−0.106).

The spatial patterns of temporal correlations between NDVI and NPP from precipitation minus runoff (Fig. 10a–c) are very similar to the spatial patterns of correlations for NPP from precipitation. Figure 10d–f shows the spatial distribution of differences between correlations, confirming that differences are small and are localised. Results for NPP calculated from precipitation therefore also hold for NPP calculated from precipitation minus runoff.

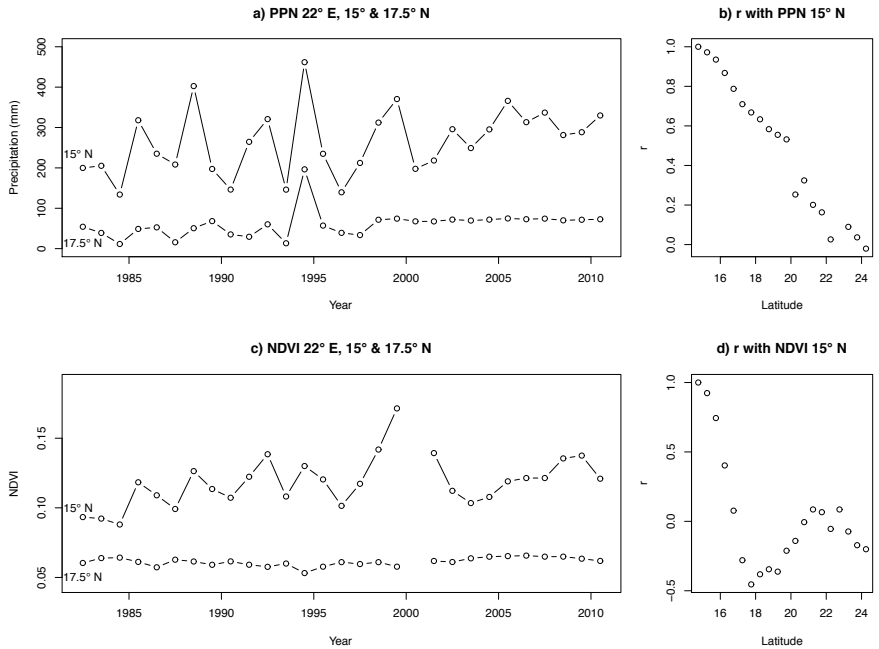

Figure 7. (a) Time series of annual precipitation for 15.25° N and 22.25° E and for 17.75° N and 22.25° E indicating a large degree of spatial correlation in precipitation across the Sahel (transition from savannah to desert south of the Sahara). **(b)** Correlation between annual precipitation at 15.25° N and 22.25° E and time series from 15.25 to 24.25° N; spatial correlation slowly decreases from 1 to 0 over a distance of approximately 780 km. **(c)** Same as **(a)** but for mean annual vegetation index time series. **(d)** Same as **(b)** but for annual vegetation index time series. The correlation between NDVI time series decreases to zero over a distance of only 280 km as opposed to 780 km for precipitation.

5 Discussion

In the present study three land-surface precipitation data sets, three land-surface precipitation reanalyses and three precipitation minus runoff reanalyses were tested. Annual precipitation and precipitation minus runoff values were converted to NPP and compared with NDVI data for 1982–2010 at latitudes between 45° S and 45° N. At these latitudes correlations between precipitation derived NPP and NDVI are high because water limits vegetation growth.

The approach adopted in the present paper, testing gridded precipitation data and reanalyses with NDVI data, is different from the more common approach where precipitation reanalyses are directly compared with precipitation data. A disadvantage of the adopted approach is that two different parameters are compared, even though these parameters are closely linked for latitudes investigated. An advantage is that the NDVI data have continuous coverage for the entire land surface and their measurement is independent of that of the precipitation data. Furthermore, the adopted approach can be extended to incorporate other components of the hydrological cycle; the residual error is expected to decrease, or at least not increase, as more components of the hydrological budget are incorporated (Eq. 3). As an example, the reanalysis precipitation minus runoff is compared with NDVI in the present study. Other components were not incorporated since runoff was the only parameter available for all reanalyses.

The NDVI data were obtained from two different satellite sensor systems; data from 1982 to 1999 were obtained from the broad-band AVHRR and data from 2001 to 2010 were obtained from the narrow-band MODIS. Different correction algorithms were applied to the two data sets; no solar zenith angle correction was applied to the MODIS data, which affects the seasonal NDVI cycle, but has a minimal effect on interannual variability. A less comprehensive correction for atmospheric effects was applied to the AVHRR data, which may lead to differences in areas where, e.g., variability in atmospheric water vapour or dust is large and is sustained for periods larger than 2 months.

Another limitation of the present study is that the NPP model does not take into account precipitation seasonality; thus, for the same annual precipitation amount, the same annual NPP is predicted for both areas with constant precipitation during the year and areas with extended dry and wet seasons.

Despite the three above limitations as well as the limitations mentioned in the discussion of Eq. (3), precipitation limited NPP values correlate well with NDVI (Figs. 3 and 6); the spatial correlations between NDVI on the one hand and NPP derived from precipitation appeared consistent across the AVHRR and MODIS records (Fig. 3). Spatial patterns and interannual variation in NDVI were reproduced to a large extent by the NPP calculated from precipitation data.

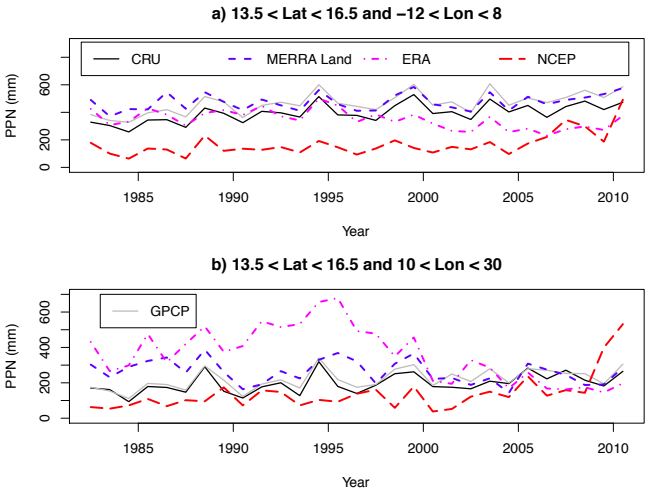

Figure 8. Precipitation time series for CRU precipitation, GPCP precipitation, MERRA Land precipitation, ERA Interim precipitation and NCEP/NCAR Reanalysis I precipitation. **(a)** For an area between 13.5–16° N and 12° W–8° E. **(b)** For an area between 13.5–16° N and 10–30° E. The ERA Interim precipitation tends to drift away from the observations over extended periods of time, whereas the NCEP/NCAR consistently underestimates the observations. Variations in the GPCP and CRU data are closely linked. GPCP data are consistently higher, likely caused by an under-catch correction applied to the data (Huffman et al., 2009; Adam and Lettenmaier, 2003).

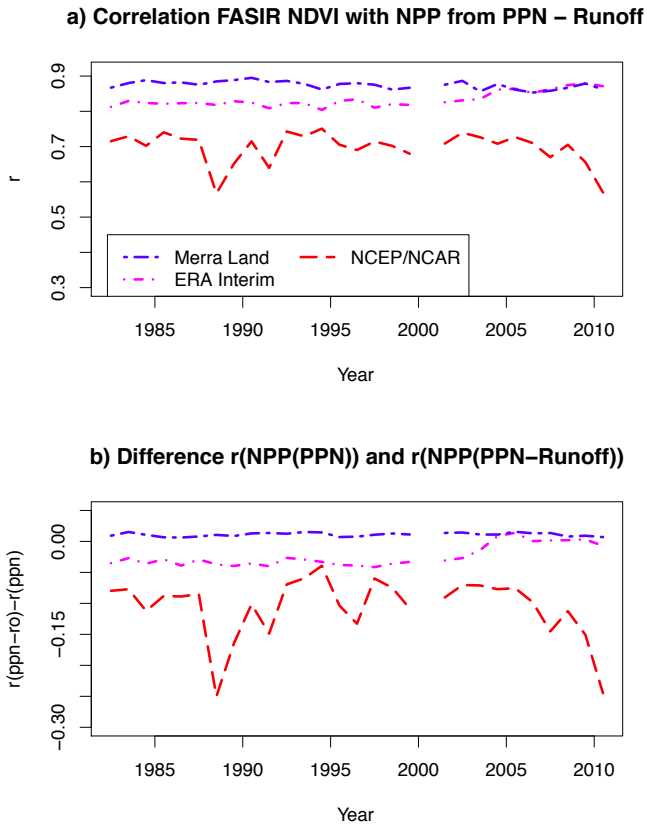

Figure 9. Evaluation of spatial agreement through time between potential annual NPP from precipitation minus runoff and mean annual NDVI.

The consistency of spatial correlations over time (Fig. 3) between NDVI and precipitation limited NPP is remarkable given that the number of stations used to obtain the CRU and GPCP data sets declines over time from more than 40 000 in 1982 to less than 10 000 in 2010. For the GPCP data the decline in the number of stations is in part compensated for by the incorporation of more accurate precipitation estimates from a newer generation of satellites (Huffman et al., 2009), but this is not the case for the CRU data.

The decline in the number of stations available for the generation of global gridded data poses a problem for the spatial and temporal analysis in the present study. It is possible to analyse only those grid cells where a sufficiently large number of stations is available. However, this would lead to a decline over time in the number of grid cells incorporated in the analysis and would make both a comparison between years difficult as well as a comparison between observed fields and reanalysis fields. The advantage in analysing the full data set is that it provides an estimate of the accuracy of entire data sets. A side analysis of the CRU data (not included in the present study) showed that the spatial correlation decreased when cells were left out based on the number of stations contributing to the gridded estimate; for example, the spatial correlation between CRU NPP and FASIR NDVI for 1992 dropped from $r = 0.893$ when all data were included to $r = 0.838$ when cells were removed, with fewer than five stations contributing to the gridded estimate.

The precipitation data and reanalysis products fall into three groups in terms of their spatial consistency with the NDVI. The first group consists of the CRU and TRMM data. This group has the highest spatial correlations. The second group consists of the GPCP data and MERRA Land and ERA Interim reanalyses with somewhat lower spatial correlation and the third group consists of the NCEP/NCAR Interim precipitation with the lowest correlation. The reduced spatial correlation of the GPCP data can be attributed to the low spatial resolution since all precipitation data show similar correlations at the (low) resolution of the NCEP/NCAR reanalysis.

The positive bias shown in the GPCP data, CRU data and TRMM data in western Africa and the Indian sub-continent (Figs. 4 and 5) could be caused either by a deficiency in the NPP model or by deficiencies in the data. An error analysis by Adler et al. (2012) of the GPCP data based on a number of independent data sets indicates that GPCP precipitation is overestimated in these parts of the world, similar to the results of the present study (compare Fig. 4 with Fig. 7 in Adler et al., 2012). A study by Dinku et al. (2008) com-

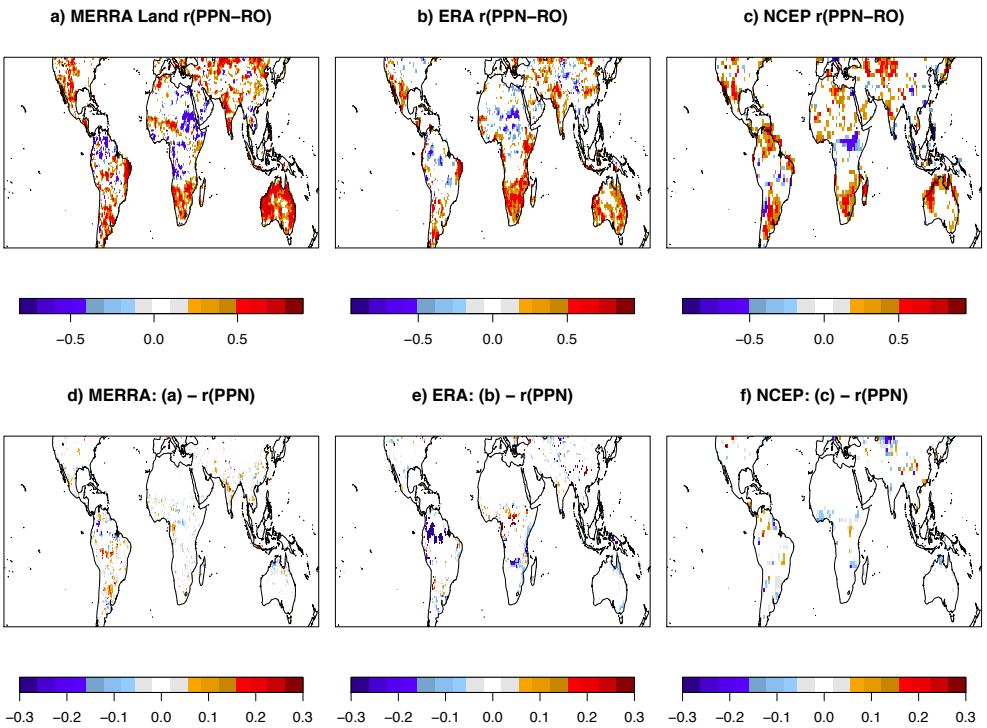

Figure 10. Spatial distributions of correlations between NDVI time series and potential NPP time series calculated from annual evapotranspiration amounts for 1982–2010 (2000 excluded). Annual evapotranspiration was estimated as precipitation–runoff. **(a)** Correlations for MERRA Land reanalysis; **(b)** correlations for ERA CE1 Interim reanalysis; **(c)** correlations for NCEP/NCAR surface Gaussian reanalysis.

paring global gridded data with data from a dense rain gauge network in eastern Africa found that CRU data overestimated precipitation in mountainous regions as a result of an overcorrection for altitude. The biases in western Africa and the Indian sub-continent were even larger in the reanalysis fields than in the observed fields.

The temporal correlation analysis divides data sets into two groups: the first consists of the gridded CRU, TRMM and GPCP data sets, which have high temporal correlations in all semi-arid regions. As an aside, the GPCP data and CRU data differ only in terms of their spatial consistency and the GPCP data can therefore be improved by increasing the spatial resolution, e.g. by using the climatology of the CRU precipitation data. The second group with lower temporal correlations consists of the MERRA, ERA Interim and NCEP/NCAR reanalyses. Correlations were realistic for semi-arid regions; however, none of the reanalysis products showed realistic interannual variations in tropical northern Africa. Even the MERRA Land precipitation showed poor correlations despite assimilation of GPCP precipitation data into this product (Reichle et al., 2011). Northern semi-arid Africa is thought to be sensitive to climate change and is likely an area where early indications of climate change are to be found. Nevertheless, modelling of temporal and spatial variability of precipitation in this area is poor and needs to be improved as a matter of urgency. In particular, the interannual variability in the ERA Interim precipitation, persisting for a number of years in a row, was much larger than observed.

Incorporation of runoff in the estimation of NPP, by calculating NPP from precipitation minus runoff, resulted in marginal improvements for the MERRA Land reanalysis. Results deteriorated by a small amount for the ERA Interim reanalysis and by a slightly larger amount for the NCEP/NCAR reanalysis. This lack of improvement likely indicates an overall weakness in the hydrological representation in land-surface models.

6 Conclusions

The CRU and TRMM precipitation data exhibit the most realistic spatial variations; the CRU, TRMM and GPCP precipitation data exhibit the most realistic temporal variations. The low spatial resolution of the GPCP data reduces realism of spatial variability.

Precipitation reanalyses exhibit realistic spatial and temporal variations for most parts of the world: the Americas, Australia, and Asia. However, spatial and temporal variations are not realistic for northern tropical Africa. Particular noteworthy problems are that extreme droughts (most notably the 1984 drought in the Sahel) are not simulated correctly. Furthermore, the interannual variability in the ERA Interim pre-

cipitation in the southern desert margin of the Sahara is too large.

ERA Interim precipitation appeared more realistic for the last 5–8 years of the record investigated.

The simulations of runoff in numerical weather forecasting models need to be improved. Only the MERRA Land reanalysis showed a modest improvement when runoff was incorporated in the calculation of NPP; other reanalysis products showed an increase in error when runoff was incorporated, indicating that errors in these simulations are large.

The proposed method, to test precipitation fields on NDVI data, can be extended to test other components of the water balance. NPP should match transpiration of water by plants most closely because of the link with carbon uptake through photosynthesis. This test was not applied since transpiration was only available for the MERRA Land reanalysis.

Acknowledgements. GPCP version 2.2 data were obtained from http://precip.gsfc.nasa.gov/; TRMM 3A12 and 3B43 version 7 data were obtained from the NASA Goddard Earth Sciences Data and Information Services Center (GES DISC) Mirador server (http://mirador.gsfc.nasa.gov). CRU version 3.21 precipitation data were obtained from the British Atmospheric Data Centre (BADC; http://badc.nerc.ac.uk/); ERA Interim reanalysis synoptic monthly means (precipitation and runoff) were obtained from http://data-portal.ecmwf.int/data/d/interim_mnth/; NCEP/NCAR daily average (Gaussian) surface precipitation reanalysis I fields were provided by the NOAA/OAR/ESRL PSD, Boulder, Colorado, USA, from their website at http://www.esrl.noaa.gov/psd/. MERRA and MERRA land reanalyses were obtained from the Goddard Earth Sciences Data and Information Services Center http://disc.sci.gsfc.nasa.gov/mdisc/. TS1Buytaert and Bergin (Imperial College London) and an anonymous reviewer are thanked for their comments and suggestions for improvement of the paper.

Edited by: W. Buytaert

References

Adam, J. C. and Lettenmaier, D. P.: Adjustment of global gridded precipitation for systematic bias, J. Geophys. Res. Atmos., 108, 4257, doi:10.1029/2002JD002499, 2003.

Adler, R. F., Gu, G., and Huffman, G. J.: Estimating climatological bias errors for the Global Precipitation Climatology Project (GPCP), J. Applied. Meteorol. Climatol., 51, 84–99, doi:10.1175/JAMC-D-11-052.1, 2012.

Berrisford, P., Dee, D., Poli, P., Brugge, R., Fielding, K., Fuentes, M., Kallberg, P., Kobayashi, S., Uppala, S., and Simmons, A.: The ERA-Interim archive Version 2.0, ERA Report Series 1, ECMWF, Shinfield Park, Reading, UK, 2011.TS2

Coenders-Gerrits, A. M. J., van der Ent, R. J., Bogaard, T. A., Wang-Erlandsson, L., Hrachowitz, M., and Savenije, H. H. G.: Uncertainties in transpiration estimates, Nature, 506, E1–E2, doi:10.1038/nature12925, 2014.

Dinku, T., Connor, S. J., Ceccato, P., and Ropelewski, C. F.: Comparison of global gridded precipitation products over mountainous regions of Africa, Int. J. Climatol., 28, 1627–1638, doi:10.1002/joc.1669, 2008.

Esser, G., Hoffstadt, J., Mack, F., and Wittenberg, U.: High Resolution Biosphere Model, Model Version 3.00.00, Tech. rep., Institute for Pland ecology, Justus-Liebig Universität, Giessen, Germany, 1994.

Harris, I., Jones, P. D., Osborn, T. J., and Lister, D. H.: Updated high-resolution grids of monthly climatic observations – the CRU TS3.10 Data set, Int. J. Climatol., 34, 623–712, doi:10.1002/joc.3711, 2014.

Huete, A., Didan, K., Miura, T., Rodriguez, E. P., Gao, X., and Ferreira, L. G.: Overview of the radiometric and biophysical performance of the MODIS vegetation indices, Remote Sens. Environ., 83, 195–213, 2002.

Huffman, G. J., Adler, R. F., Morrissey, M. M., Bolvin, D. T., Curtis, S., Joyce, R., McGavock, B., and Susskind, J.: Global precipitation at one-degree daily resolution from multisatellite observations, J. Hydrometeorol., 2, 36–50, doi:10.1175/1525-7541(2001)002<0036:GPAODD>2.0.CO;2, 2001.

Huffman, G. J., Adler, R. F., Bolvin, D. T., Gu, G., Nelkin, E. J., Bowman, K. P., Hong, Y., Stocker, E. F., and Wolff, D. B.: The TRMM multi-satellite precipitation analysis: quasi-global, multi-year, combined-sensor precipitation estimates at fine scale, J. Hydrometeorol., 8, 38–55, doi:10.1175/JHM560.1, 2007.

Huffman, G. J., Adler, R. F., Bolvin, D. T., and Gu, G.: Improving the global precipitation record: GPCP Version 2.1, Geophys. Res. Lett., 36, L17808, doi:10.1029/2009GL040000, 2009.

Huffman, G. J., Adler, R. F., Bolvin, D. T., and Nelkin, E. J.: Satellite Rainfall Applications for Surface Hydrology, chap. 1, The TRMM Multi-satellite Precipitation Analysis (TMPA), Springer Verlag, 2010. TS3

Huffman, G. J., Bolvin, D. T., and Adler, R. F.: GPCP Version 2.2 Combined Precipitation Data Set, available at: http://precip.gsfc.nasa.gov/gpcp_v2.2_data.html (last access date: 1 August 2012), 2011.

James, M. E. and Kalluri, S. N. V.: The Pathfinder AVHRR land data set – an improved coarse resolution data set for terrestrial monitoring, Int. J. Remote Sens., 15, 3347–3363, 1994.

Jasechko, S., Sharp, Z. D., Gibson, J. J., Birks, S. J., Yi, Y., and Fawcett, P. J.: Terrestrial water fluxes dominated by transpiration, Nature, 496, 347–351, doi:10.1038/nature11983, 2013.

Jasechko, S., Sharp, Z. D., Gibson, J. J., Birks, S. J., Yi, Y., and Fawcett, P. J.: Jasechko et al. reply, Nature, 506, E2–E3, doi:10.1038/nature12926, 2014.

Jonas, P.: Turbulence and cloud microphysics, Atmos. Res., 40, 283–306, doi:10.1016/0169-8095(95)00035-6, 1996.

Kalnay, E., Kanamitsu, M., Kistler, R., Collins, W., Deaven, D. Gandin, L., Iredell, M., Saha, S., White, G., Woollen, J., Zhu, Y., Leetmaa, A., Reynolds, R., Chelliah, M., Ebisuzaki, W., Higgins, W., Janowiak, J., Mo, K. C., Ropelewski, C., Wang, J., Jenne, R., and Joseph, D.: The NCEP/NCAR 40-Year Reanalysis Project, B. Amer. Meteorol. Soc., 77, 437–471, doi:doi:10.1175/1520-0477(1996)077<0437:TNYRP>2.0.CO;2, 1996.

Kumar, M. and Monteith, J. L.: Remote sensing of crop growth, in: Plants and the Daylight Spectrum, edited by: Smith, H., Academic Press, London, 133–144, 1981.

Los, S. O.: Calibration adjustment of the NOAA Advanced Very High Resolution Radiometer without recourse to component

channel-1 and channel-2 data, Int. J. Remote Sens., 14, 1907–1917, 1993.

Los, S. O.: Estimation of the ratio of sensor degradation between NOAA AVHRR channels 1 and 2 from monthly NDVI composites, IEEE T. Geosci. Remote, 36, 206–213, doi:10.1109/36.655330, 1998.

Los, S. O.: Analysis of trends in fused AVHRR and MODIS NDVI data for 1982–2006: indication for a CO_2 fertilization effect in global vegetation, Global Biogeochem. Cy., 27, 318–330, doi:10.1002/gbc.20027, 2013.

Los, S. O., Collatz, G. J., Sellers, P. J., Malmström, C. M., Pollack, N. H., DeFries, R. S., Bounoua, L., Parris, M. T., Tucker, C. J., and Dazlich, D. A.: A global 9 yr biophysical land surface data set from NOAA AVHRR data, J. Hydrometeorol., 1, 183–199, 2000.

Los, S. O., North, P. R. J., Grey, W. M. F., and Barnsley, M. J.: A method to convert AVHRR Normalized Difference Vegetation Index time series to a standard viewing and illumination geometry, Remote Sens. Environ., 99, 400–411, doi:10.1016/j.rse.2005.08.017, 2005.

Malmström, C., Thompson, M., Juday, G., Los, S., Randerson, J., and Field, C.: Interannual variation in global-scale net primary production: testing model estimates, Global Biochem. Cy., 11, 367–392, 1997.

Potter, C. S., Randerson, J. T., Field, C. B., Matson, P. A., Vitousek, P. M., Mooney, H. A., and Klooster, S. A.: Terrestrial ecosystem production: a process model based on global satellite and surface data., Global Biogeochem. Cy., 7, 811–841, 1993.

Randall, D. A.: Beyond deadlock, Geophys. Res. Lett., 40, 5970–5976, doi:10.1002/2013GL057998, 2013.

Reichle, R. H., Koster, R. D., De Lannoy, G. J. M., Forman, B. A., Liu, Q., Mahanama, S. P. P., and Toure, A.: Assessment and enhancement of MERRA land surface hydrology estimates, J. Climate, 24, 6322–6338, doi:10.1175/JCLI-D-10-05033.1, 2011.

Schlesinger, W. H. and Jasechko, S.: Transpiration in the global water cycle, Agr. Forest Meteorol., 189–190, 115–117, doi:10.1016/j.agrformet.2014.01.011, 2014.

Sellers, P. J., Los, S. O., Tucker, C. J., Justice, C. O., Dazlich, D. A., Collatz, G. J., and Randall, D. A.: A Revised Land-Surface Parameterization (SiB2) for Atmospheric GCMs. Part 2: The generation of global fields of terrestrial biophysical parameters from satellite data, J. Climate, 9, 706–737, 1996.

Tucker, C. J. and Sellers, P. J.: Satellite remote sensing of primary production, Int. J. Remote Sens., 7, 1395–1416, 1986.

Vermote, E. F., Justice, C. O., Descloitres, J., El Saleous, N., Roy, D. P., Ray, J., Margerin, B., and Gonzalez, L.: A SeaWiFS global monthly coarse-resolution reflectance data set, Int. J. Remote Sens., 22, 1151–1158, 2001.

Remarks from the language copy-editor

CE1 For consistency with the rest of the paper

Remarks from the typesetter

TS1 Please add first name initials of Buytaert and Bergin.
TS2 Please add page range if available.
TS3 Please add page range if available.